ARCHIVES OF ELECTRICAL ENGINEERING VOL. 68(2), pp. 237–244 (2019)

DOI 10.24425/aee.2019.128265

Transient approach for iron loss separation of non-grain-oriented electrical steels considering the impact of cut edge effect

CHRISTOPH MÜLDER, SILAS ELFGEN, KAY HAMEYER

RWTH Aachen University, Institute of Electrical Machines, Germany
e-mail: {christoph.muelder/silas.elfgen/kay.hameyer}@rwth-aachen.de

(Received: 28.09.2018, revised: 02.11.2018)

Abstract: The purpose of this paper is to focus on the loss separation of non-grain-oriented electrical steels used for speed-variable rotating electrical machines. The impact of laser-cutting, used in prototype manufacturing and of flux density harmonics, occurring locally in the lamination, on the loss distribution is studied in detail. Iron losses occurring under operation can physically be separated in different loss components. In this paper, a frequency-based loss model with parameters identified for single-sheet tester specimens, cut in strips of different widths, is therefore used. Moreover, a time-domain approach considers loss distributions occurring from higher harmonics. Hysteresis losses having high sensitivity to cut edge effects are calculated by the well-known Jiles-Atherton model adapting the frequency-based loss parameters. The model is validated by free-curve measurements at a single-sheet tester. It has been shown that the studied elliptical hysteresis model becomes inaccurate particularly for specimens with small strip widths with similar dimensions as teeth of electrical machine laminations. The incorrect mapping of losses occurring from minor hysteresis loops due to higher harmonics is concluded. The results show consequently that both, the impact of a cut edge effect and local distributions of flux density harmonics need to be considered in terms of accurate iron loss prediction of electrical machine design.

Key words: cut edge effect, hysteresis losses, iron losses, transient loss model

1. Introduction

The efficiency quantification of rotating electrical machines by simulation requires accurate loss models in the development stage. Nowadays, highly utilized electrical machines can have a significant share in the total losses, particularly during high speed. Therefore, a precise modelling of the soft-magnetic materials used for the lamination is essential in this context. Laser cutting is an often-used processing technique for prototype manufacturing. The local heating and the following abrupt cooling of the lamination induce thermal residual stress in the vicinity of the cut edge [1].

This can lead to a stronger deterioration of the magnetizability and the loss behaviour when compared to other mechanical cutting techniques e.g. such as stamping [2].

Since iron losses originate from different micro- and macroscopic mechanisms, the impact of thermal stress induced by laser cutting on loss components is studied in this paper.

Because of the small geometrical dimensions within a low power electrical machine (e.g. 8 mm) the ratio of damaged material is high, resulting in a significant impact of cut edges on the local loss behaviour. Magnetic flux densities with high harmonic content appear locally in electrical machines producing additional loss contributions. Based on the parameters from a frequency-dependent iron loss model [2, 3], both the effects of higher harmonics and manufacturing influences are considered in a separation approach using a time domain model.

2. Theory

The IEM-formula for alternating magnetic flux densities separates the total iron loss density p_{Fe} [W/kg] in dependence of the amplitude B and frequency f in four components [4]:

$$p_{\text{Fe}} = p_{\text{hyst}} + p_{\text{eddy}} + p_{\text{nl}} + p_{\text{excess}} = a_1 B^{\alpha} f + a_2 (Bf)^2 \cdot (1 + a_3 B^{a_4}) + a_5 (Bf)^{1.5}, \tag{1}$$

where: a_1 and α are the hysteresis, a_2 is the classical eddy current, a_3, a_4 represent the non-linear and a_5 the excess loss parameters.

The model allows accurate loss prediction also for flux densities towards the saturation region above 1.5 T and high frequencies (> 400 Hz). The loss parameters are identified on single-sheet specimens of different widths, to quantify the cut edge impact. In [5] a dynamic iron loss model depending on the flux density waveform $B(t)$ and its derivative $\mathrm{d}B/\mathrm{d}t$ is proposed:

$$p_{\text{Fe}}(t) = p_{\text{hyst}}(t) + p_{\text{eddy}}(t) + p_{\text{excess}}(t), \tag{2}$$

where the hysteresis loss component is described by the irreversible component of the magnetic field strength

$$p_{\text{hyst}}(t) = H_{\text{irr}}(t) \frac{\mathrm{d}B}{\mathrm{d}t}, \tag{3}$$

with

$$H_{\text{irr}}(t) = \frac{k_{\text{hyst}} \rho B_{\max}}{C_{\beta}} \left(\sqrt{1 - \left(\frac{B(t)}{B_{\max}} \right)^2} \right)^{\beta - 1} \tag{4}$$

and

$$C_{\beta} = 4 \int\limits_0^{\frac{\pi}{2}} \cos^{\beta}(\theta)\, \mathrm{d}\theta. \tag{5}$$

In (4) $B_{\max}$ is the maximum of the magnetic flux density over one period and ρ is the specific density of the material.

k_{hyst} and β are equal to the hysteresis loss parameters a_1 and α in (1). This elliptical approach for the hysteresis loss calculation in the time domain separates the magnetic flux density in a reversible and irreversible component according to (4). The resulting waveforms are illustrated in Figure 1.

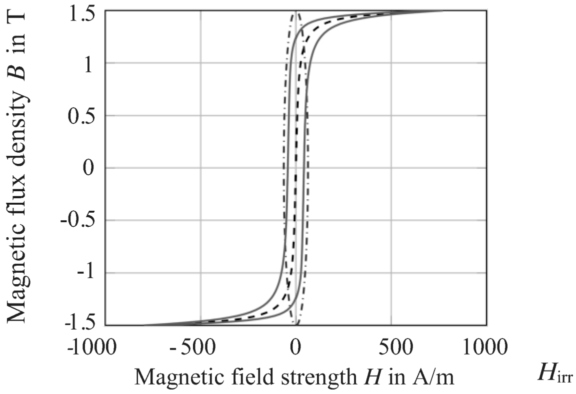

Fig. 1. Separation of the magnetic field strength in reversible and irreversible component

In the dynamic model the classical eddy current losses p_{eddy} and the anomalous eddy current (excess) losses p_{excess} are given by:

$$p_{\mathrm{eddy}}(t) = \frac{k_{\mathrm{eddy}}}{2\pi^2}\left|\frac{\mathrm{d}B}{\mathrm{d}t}\right|^2, \tag{6}$$

$$p_{\mathrm{excess}}(t) = \frac{k_{\mathrm{excess}}}{C_{\mathrm{excess}}}\left|\frac{\mathrm{d}B}{\mathrm{d}t}\right|^{1.5}, \tag{7}$$

where k_{eddy} that is equivalent to a_2 can be calculated by the specific conductivity, thickness and specific density of the material is constant for all specimens [6] and $C_{\mathrm{excess}} \approx 8.763$.

Since the loss model (1) in the frequency domain contains a non-linear term, an equivalent in the time domain is introduced:

$$p_{\mathrm{nl}}(t) = \frac{a_2}{2\pi^2} a_3 B_{\max}^{a_4}\left|\frac{\mathrm{d}B}{\mathrm{d}t}\right|^2, \tag{8}$$

where: a_3 and a_4 equal the non-linear loss parameters in (1).

Besides the explained elliptical approach for the modeling of static hysteresis losses, the Jiles-Atherton model in reverse form is introduced [7]:

$$\frac{\mathrm{d}M}{\mathrm{d}B} = \frac{\delta_M (M_{\mathrm{an}} - M) + \delta c k \dfrac{\mathrm{d}M_{\mathrm{an}}}{\mathrm{d}H_{\mathrm{e}}}}{\mu_0\left(\delta k + (1-\alpha_{\mathrm{J.A.}})\left[\delta_{\mathrm{M}}(M_{\mathrm{an}} - M) + \delta c k \dfrac{\mathrm{d}M_{\mathrm{an}}}{\mathrm{d}H_{\mathrm{e}}}\right]\right)}, \tag{9}$$

where the anhysteretic magnetization M_{an} depending on the effective field strength

$$H_{\mathrm{e}} = H + \alpha_{\mathrm{J.A.}} M, \tag{10}$$

with the parameter $\alpha_{\mathrm{J.A.}}$ can be calculated analytically [8].

The irreversible component of the magnetic field strength in (3) is replaced by the solution $H_{\mathrm{J.A.}}$ of the model. This is gained by the differential equation with the differential $\mathrm{d}M/\mathrm{d}B$ for the magnetization M:

$$\frac{\mathrm{d}H_{\mathrm{J.A.}}}{\mathrm{d}t} = \frac{1}{\mu_0}\frac{\mathrm{d}B}{\mathrm{d}t}\left(1 - \frac{\mathrm{d}M}{\mathrm{d}B}\right), \tag{11}$$

where μ_0 is the vacuum permeability.

3. Measurements

The material specimens are produced of non-grain-oriented steel of grade M400-50A typically used for the laminations of rotating electrical machines. For the measurement 120 mm wide and long single-sheet tester specimens were cut by a CO_2 laser parallel and perpendicular to the rolling direction in strips of 60, 20, 10, 5 and 4 mm width. Two specimens are left uncut as a reference of undamaged material behaviour.

The specimens are magnetically characterized according to the IEC standard 60404-4 using a single-sheet tester (SST), the field-metric method. For the loss separation of the specimens, a standard measurement procedure was performed with sinusoidal magnetic flux density waveforms with frequencies from 0.1 Hz (quasi-static) up to 800 Hz and amplitudes from 0.1 T to 1.8 T.

To analyse the accuracy of the dynamic loss model for flux density waveforms with higher harmonic content, free-curve measurements were performed in addition. The local field solutions in the tooth tip of an induction machine extracted from FE-simulations serve as a basis for the analysis of the loss models. In Figure 2(a), the radial flux density in a tooth tip of the stator is illustrated (dashed curve). The waveform was imposed at the SST for all specimens as reference value. Due to the limited dynamics of the SST-controller, the measured waveform (solid curve)

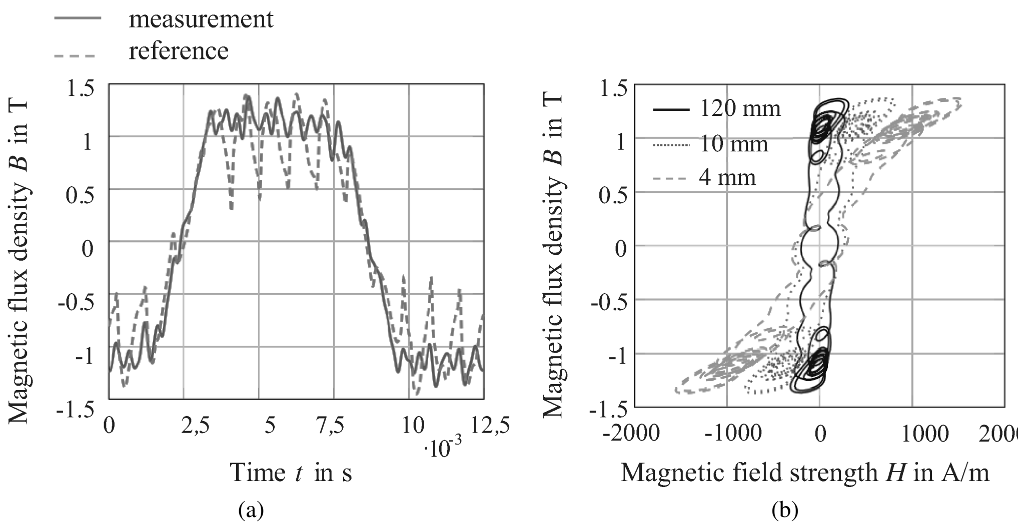

Fig. 2. Flux density waveform measured by SST and of reference extracted from FE-data (a); hysteresis loops of measurement for specimens with different strip widths (b)

deviates from it. It contains harmonic content though and can be analysed qualitatively in terms of the loss separation for this reason.

In Figure 2(b) the measured hysteresis loops of the presented free-curve excitation mode of the SST device exemplary for three specimens with different strip widths are illustrated. Besides the shearing and expansion of the hysteresis loop due to the impact of cut edges, the occurrence of minor hysteresis loops is observed.

The impact on the loss distribution, particularly on the hysteresis losses, of the specimens with a different amount of cut edge-length, is studied in detail.

4. Results

In Figure 3 the results for the identified hysteresis loss parameters a_1 and α from (11) of the studied material specimens cut parallel and perpendicular to the rolling direction (RD) are illustrated. Quasi-static measurements for flux density levels between 0.1 and 1.6 T were used for the identification.

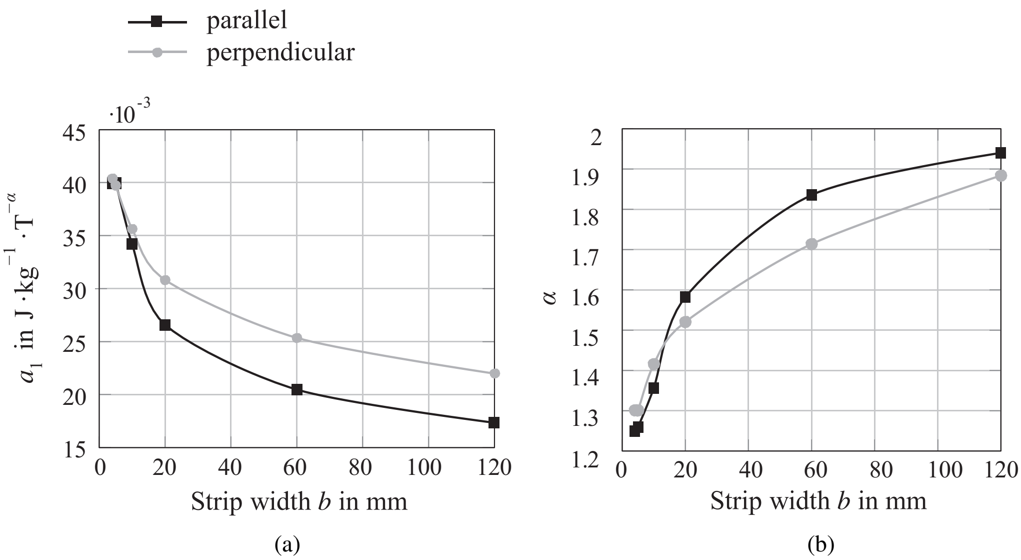

Fig. 3. Hysteresis loss parameter a_1 and α for specimens cut parallel and perpendicular to RD in different strip widths

In accordance to other works [9] the parameters show a significant sensitivity to cut edge effects, since a_1 increases monotonically with decreasing strip width. The impact of the magnetization direction reduces and disappears approximately for the specimens with a smallest strip width of 5 and 4 mm respectively.

The quadratic relation proposed by Steinmetz that fits for undamaged material specimens with widths of 120 mm becomes linear for an increasing degradation of the material as α decreases with the strip width.

The other loss parameters from the separation approach (1) are identified analogously for different flux density and frequency levels and are adapted in the dynamic loss model according to (3)–(8). The results for iron loss densities of the flux density waveform represented in Figure 2 for the measurement and model are illustrated in Figure 4(a).

The model deviates sharply for all samples tested with different strip widths from the measurement. Besides the significant contribution of eddy current losses because of the applied harmonic flux densities, the loss separation shows large proportions of hysteresis losses.

In Figure 5 the result for the fitting of the hysteresis loop is illustrated. The model fit deviates slightly from the measurement, though the difference between the hysteresis energies is smaller than 3%. Consistently, the model is used as an alternative for the transient description of static hysteresis losses. As shown in other work [7], the model is able to calculate minor loops occurring under arbitrary waveforms and can, therefore, be used for the scope of this discourse.

For the calculation of the hysteresis loss distributions in the remaining specimens with a different number of cut edges, the results of the frequency-based parameter identification from the sinusoidal waveforms (Figure 3) are adapted.

A scaling approach with the sample specific loss parameters from the frequency domain $a_1(b)$ and $\alpha(b)$ is used to consider the impact of cut edge effect:

$$p_{\text{hyst, J.A.}}(t, b) = \frac{a_1(b) B_{\max}^{\alpha(b)}}{a_{1,\text{ ref.}} B_{\max}^{\alpha_{\text{ref.}}}} p_{\text{hyst., J.A., ref.}}(t), \tag{12}$$

where $a_{1,\text{ ref.}}$ and $\alpha_{\text{ref.}}$ are the loss parameters of the reference specimen.

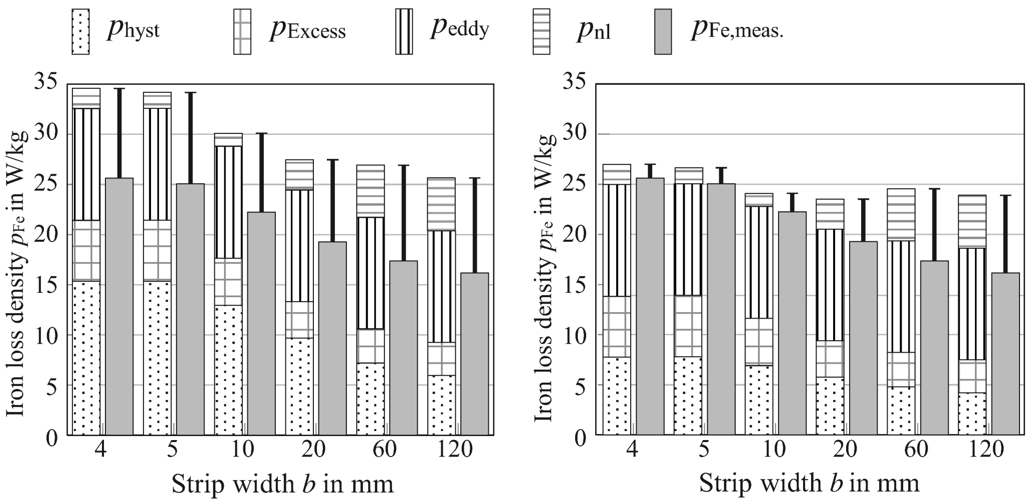

Fig. 4. Iron loss density from measurement, model with elliptical (a) and scaled Jiles-Atherton (b) hysteresis model (12)

As illustrated in Figure 4(b), the measured and calculated iron loss densities are predicted more accurately compared to the elliptical approach. Especially the specimens with small strip widths are in better agreement, since the shares of static hysteresis losses are smaller.

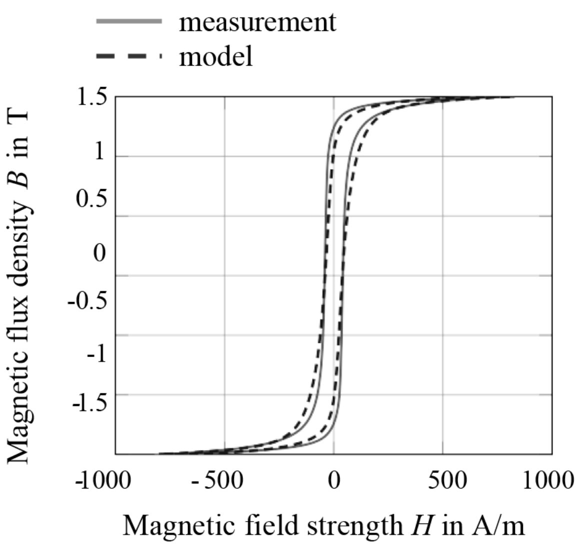

Fig. 5. Static hysteresis loop of lengthwise cut reference probe (b = 120 mm) from measurement and Jiles-Atherton model

The residual deviation of the specimens with broader strips, and consequently a fewer number of cut edges, results from the analytical eddy current loss formula, since it becomes inaccurate for high magnetizing frequencies as studied in other work [10].

5. Conclusions

In this paper, a transient approach for the separation of iron losses in non-grain-oriented electrical steel occurring under flux density waveforms with higher harmonic content that considers the impact of a cut edge effect is discussed. Therefore, measurements of sinusoidal and free-curve uniaxial flux density waveforms have been performed on a single-sheet tester for specimen dimensions of 120 × 120 mm. Material specimens, on the one hand cut into parallel as well as on the other hand cut into perpendicular strips of different widths, were used to study the impact of the cut edge effect.

The measurement results of sinusoidal flux density waveforms have yielded the parameter identification for a frequency-based loss model depending on the flux density amplitude and frequency.

The dynamic loss model in time domain with an elliptical hysteresis loss description uses those parameters and was applied to free-curve measurements. It has been shown that the described approach becomes inaccurate especially for specimens with high amount of cut edges.

An incorrect mapping of losses occurring from minor hysteresis loops due to higher harmonics is concluded. Therefore, a scaling approach of the inverse Jiles-Atherton model adapting frequency based parameters is proposed and leads to an improved accuracy, especially for specimens that are magnetically influenced by cut edges.

The presented results show that both the impact of cut edge effect and local distributions of flux density harmonics need to be considered in terms of accurate iron loss prediction of electrical machine design.

By using physically based hysteresis models such as Jiles-Atherton model in addition to loss parameters identified on small specimen geometries, an improved understanding and modeling of non-linear phenomena occurring in those machines can be achieved.

References

[1] Siebert R., Schneider J., Beyer E., *Laser Cutting and Mechanical Cutting of Electrical Steels and its Effect on the Magnetic Properties*, IEEE Transactions on Magnetics, vol. 50, no. 4, pp. 1–4 (2014).

[2] Steentjes S., Leßmann M., Hameyer K., *Semi-physical parameter identification for an iron-loss formula allowing loss-separation*, Journal of Applied Physics, vol. 113, no. 17 (2013).

[3] Steentjes S., Eggers D., Leßmann M., Hameyer K., *Iron-loss model for the FE-simulation of electrical machines*, INDUCTICA TECHNICAL CONFERENCE, CWIEME Berlin, pp. 239–246 (2012).

[4] Steentjes S., Eggers D., Leßmann M., Hameyer K., *Iron-loss model for the FE-simulation of electrical machines*, INDUCTICA TECHNICAL CONFERENCE, CWIEME Berlin, pp. 239–246 (2012).

[5] Lin D., Zhou P., Fu W.N., Badics Z., Cendes Z.J., *A dynamic core loss model for soft ferromagnetic and power ferrite materials in transient finite element analysis*, IEEE Transactions on Magnetics, vol. 40, no. 2, pp. 1318–1321 (2004).

[6] Hofmann M., Naumoski H., Herr U., Herzog H.G., *Magnetic Properties of Electrical Steel Sheets in Respect of Cutting: Micromagnetic Analysis and Macromagnetic Modeling*, IEEE Transactions on Magnetics, vol. 52, no. 2, pp. 1–14 (2016).

[7] Steentjes S., Hameyer K., Dolinar D., Petrun M., *Iron-Loss and Magnetic Hysteresis Under Arbitrary Waveforms in NO Electrical Steel Sheets: A Comparative Study of Hysteresis Models*, IEEE Transactions on Industrial Electronics, vol. PP, no. 99, p. 1 (2016).

[8] Kokornaczyk E., Gutowski M.W., *Anhysteretic Functions for the Jiles-Atherton Model*, IEEE Transactions on Magnetics, vol. 51, no. 2, pp. 1–5 (2015).

[9] Elfgen S., Steentjes S., Böhmer S., Franck D., Hameyer K., *Continuous Local Material Model for Cut Edge Effects in Soft Magnetic Materials*, IEEE Transactions on Magnetics, vol. 52, no. 5, pp. 1–4 (2016).

[10] Zirka S., Moroz Y., Marketos P., Moses A., *Evolution of the loss components in ferromagnetic laminations with induction level and frequency*, Journal of Magnetism and Magnetic Materials, vol. 320, no. 20, pp. 1039–1043 (2008).